J|A|C|S
ARTICLES
Published on Web 11/23/2004

Donor-Mediated Band Gap Reduction in a Homologous Series of Conjugated Polymers

Christopher A. Thomas,[†,‡] Kyukwan Zong,[†,⊥] Khalil A. Abboud,[†] Peter J. Steel,[§] and John R. Reynolds*[,†]

Contribution from the Department of Chemistry and Center for Macromolecular Science and Engineering, University of Florida, Gainesville, Florida 32611-7200, and University of Canterbury, Christchurch, New Zealand

Received March 9, 2004; E-mail: reynolds@chem.ufl.edu

Abstract: A family of six donor−acceptor−donor monomers was synthesized using combinations of thiophene, 3,4-ethylenedioxythiophene and 3,4-ethylenedioxypyrrole as donor moieties, and cyanovinylene as the acceptor moiety, to understand the effects of modified donor ability on the optoelectronic and redox properties of the resulting electropolymerized materials. Spectroelectrochemistry, differential pulse voltammetry, and cyclic voltammetry results indicate band gaps ranging from 1.1 to 1.6 eV and suggest that these polymers can be both p-type and n-type doped at accessible potentials. *In situ* conductivity results indicate that the n-type conductivity magnitude is modest, and the conductivity profile indicates a redox conductivity mechanism as opposed to a delocalized electronic band mechanism as observed for p-type doping.

Introduction

The evolution of the field of conjugated electroactive polymers (CEPs) as replacements for inorganic materials in electronic devices has been fueled by the flexibility in tailoring specific electronic properties by chemical synthesis. To this end, several examples of organic light emitting, photovoltaic,[1] field effect transistor (FET),[2] and electrochromic devices[3] continue to be developed.[4] The unique properties of CEPs are largely based on the ability to tailor the energy levels of the valence band (VB) and conduction band (CB), both relative to each other (band gap control) or in an absolute sense (modifying the ease of oxidation or reduction). Tailoring the band gap (E_g) of CEPs allows variation in emission wavelength, absorptive colors in electrochromic devices, and conductivity in the neutral state. Changes in band energy allow optimization of interfacial energy level alignment between the polymer and electrode contacts in organic light emitting devices (OLEDs) and thin-film transistors (TFTs).[5] Low band gap CEPs are particularly interesting because of the possibility of high intrinsic conductivity in the neutral state, transparency in the p-doped conducting state, and their tendency to achieve reduced band gaps through conduction band energy lowering potentially leading to stable n-type doping. The factors that affect band gap have been reviewed.[6] The present contribution examines the role of donor heterocycles of varying strength for use in band gap reduction of a family of donor−acceptor polymers. These factors are examined exclusive of the other controlling elements that affect band gap such as acceptor strength, planarity of the repeat unit, resonance contributions, bond-length alternation, and interchain effects.

The donor−acceptor route has the most utility in terms of diversity in synthetic possibilities while avoiding the solubility problems that plague planar organic molecules. The route described in this contribution is formally a donor−acceptor−donor (D−A−D) route since the desire to electropolymerize these monomers enforces the condition that easily oxidized and electropolymerizable heterocycles are at the ends of the monomer. Furthermore, the general donor−acceptor approach can be loosely classified into two distinct families of monomers: those for which resonance structures can be drawn that include the acceptor group and main chain polymer conjugation together and those which use the acceptor to inductively modify the backbone. In complementary work, we have altered the acceptor strength in a family of D−A−D polymers which utilized dioxythiophenes as the donor and pyridine or pyridopyrazine as the acceptor.[7] It is generally accepted that the HOMO of the donor

[†] University of Florida.
[‡] Current address: Abbott Laboratories, 1360 South Loop Rd., Alameda, CA 94502.
[⊥] Permanent address: Department of Chemistry, Chonbuk National University, Jeonju, Korea.
[§] University of Canterbury.

(1) (a) Ramos, A. M.; Rispens, M. T.; van Duren, J. K. J.; Hummelen, J. C.; Janssen, R. A. J. *J. Am Chem. Soc.* **2001**, *123*, 6714−6715. (b) Manoj, A. G.; Alagiriswamy; Narayan, K. S. *J. Appl. Phys.* **2003**, *94*, 4088−4095.
(2) Meijer, E. J.; De Leeuw, D. M.; Setayesh, S.; van Veenendaal, E.; Huisman, B.-H.; Blom, P. W. M.; Hummelen, J. C.; Scherf, U.; Klapwijk, T. M. *Nat. Mater.* **2003**, *2*, 678−682.
(3) (a) van Mullekom, H. A. M.; Vekemans, J. A. J. M.; Havinga, E. E.; Meijer, E. W. *Mater. Sci.Eng.* **2001**, *32*, 1−40. (b) Groenendaal, L. B.; Jonas, F.; Freitag, D.; Pielartzik, H.; Reynolds, J. R. *Adv. Mater.* **2000**, *12*, 481−494. (c) de Leeuw, D. *Phys. World* **1999**, 31. (d) Friend, R. H.; Gymer, R. W.; Holmes, A. B.; Burroughes, J. H.; Marks, R. N.; Taliani, C.; Bradley, D. D. C.; Dos Santos, D. A.; Brédas, J. L.; Lögdlund, M.; Salaneck, W. R. *Nature* **1999**, *397*, 121−128.
(4) (a) Meng, H.; Tucker, D.; Chaffins, S.; Chen, Y.; Helgeson, R.; Dunn, B.; Wudl, F. *Adv. Mater*. **2003**, *15*, 146−149. (b) Ishii, H.; Sugitama, K.; Ito, E.; Seki, K. *Adv. Mater*. **1999**, *11*, 605−625.
(5) Fachetti, A.; Yoon, M.-H.; Stern, C. L.; Katz, H. E.; Marks, T. J. *Angew. Chem., Int. Ed.* **2003**, *42*, 3900−3903.
(6) Roncali, J. *Chem. Rev.* **1997**, *97*, 173−206.

10.1021/ja048637w CCC: $27.50

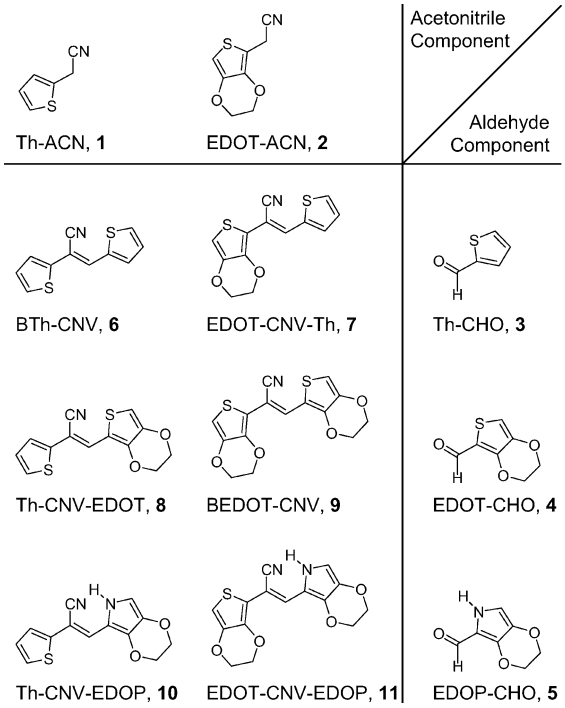

Figure 1. Matrix illustrating varied donor strength in D−A−D monomers based on cyanovinylenes. An aromatic acetonitrile is condensed with an aromatic carboxaldehyde with KO*t*Bu in ethanol to afford six monomers.

heterocycle contributes strongly to the polymer VB and the LUMO of the acceptor heterocycle determines the CB energy.

Here, the synthesis of a matrix of structurally homologous conducting polymers, differing systematically in the density of electron-rich chromophore in direct conjugation with a cyanovinylene acceptor containing polymer backbone, is described. In addition, the effect of increasing the electron-rich character along the polymer main chain is detailed. This approach is an effective method for decreasing the band gap along a polymer chain and lends insight into techniques for modifying the electronic properties of conjugated materials in general. In this work, the generally held assumption that acceptor strength must continually increase in order to decrease the band gap of a conjugated polymer is challenged.[8] Moreover, our approach to creating the acceptor unit through the high-yielding Knoevenagel condensation has general applicability to the synthesis of a variety of high molecular weight, conjugated step-growth condensation polymers which are soluble and processible for use in OLEDs and photovoltaic devices.[9]

Results

Monomer Synthesis and Structure. Access to the cyanovinylene monomers was afforded by Knoevenagel condensation of an aromatic carboxaldehyde premonomer (**3**, **4**, or **5**) with an aromatic acetonitrile moiety (**1** or **2**) in refluxing ethanol (**6**−**9**) or *tert*-butyl alcohol (**10**, **11**) containing potassium *tert*-butoxide as shown in Figure 1. The 3,4-ethylenedioxythiophene (EDOT) or 3,4-ethylenedioxypyrrole (EDOP) containing premonomer carboxaldehydes[10] (**4**, **5**) and acetonitrile (**2**) were prepared by analogy to known synthetic routes. The structural diversity of this family is due to the combination of three aromatic carboxaldehydes with two aromatic acetonitriles allowing the preparation of six monomers with a cyanovinylene central acceptor. The inclusion of the EDOP unit and its ability to react by Vilsmeier chemistry to form EDOP carboxaldehyde,[11] **5**, increases the structural variety of the monomers available. The Knoevenagel condensation of an aromatic aldehyde with an aromatic acetonitrile is used as the last step in monomer synthesis with simultaneous preparation of the cyanovinylene core and routinely allows for unoptimized yields of 80−95%. The inability to prepare the EDOP−acetonitrile analogue precluded preparation of the EDOP moiety α to the cyano group.

The electron-rich character for the three heterocycle cores in this work follows the trend EDOP > EDOT > Th as evidenced by their oxidation potentials when they are homopolymerized. Evidence that EDOP is considerably more electron rich than EDOT is noticeable as solutions of EDOP readily polymerize on standing in air to form deep blue/purple solutions, while EDOT undergoes some initial chemistry but does not form dark solutions. Monomer UV−vis spectra (see Supporting Information) show that λ_{max} increases from **6** through **11** with a total 37 nm red shift. These follow the expected trend, where the less electron-rich monomers have blue-shifted λ_{max} values.

X-ray structure results for the crystallizable monomers are shown in Figure 2 and indicate that planarity is the dominant feature throughout this family as angles formed by the plane of the cyanovinylene unit with the plane of the sp^2 hybridized heterocycle atoms in either ring is less than 9° in all cases except for **11**,[12] where the angle formed by the EDOP ring and cyanovinylene unit is 21.9°. Monomer **6** crystallizes with disorder in the crystal structure resulting from the molecule being flipped end for end at random sites. By contrast, the crystal structure of **7** has the thiophene ring disordered over two unequally occupied (79:21) orientations where the major contributor in the disordered structure has the sulfur of the thiophene ring cisoid to the vicinal nitrile group, as is the case for the heteroatom within the heterocycle β to the nitrile group in all five structures. The sulfur atom of the EDOT ring is also cisoid to the geminal nitrile group, as it is in compound **11**. This is in contrast to the structures of **6**, **8**, and **10**, which contain α thiophene rings with the sulfurs transoid to the nitrile groups.

Electropolymerization. As is typical of conjugated molecules containing thiophene or pyrrole with unblocked 2 or 5 positions, these monomers oxidizatively polymerize to form redox-active, electrode-confined films on Pt, Au, glassy carbon, and ITO. This polymerization proceeds without overt control of regiospecificity, and the possibilities are shown in Figure 3A,C for the polymer resulting from polymerization of **7**. Ring A is defined as the heterocycle α to the cyano group which stems from the heterocyclic acetonitrile premonomer (**1**, **2**). Ring B stems from the aldehyde component (**3**−**5**). The crystal structure for a dimer of EDOT[13] is shown in Figure 3B, and it should be

(7) (a) Irvin, D. J.; DuBois, C. J.; Reynolds, J. R. *Chem. Commun.* **1999**, 2121−2122. (b) DuBois, C. J.; Reynolds, J. R. *Adv. Mater.* **2002**, 1844−1846.
(8) (a) Brédas, J.-L.; Cornil, J.; Beljonne, D.; Dos Santos, D. A.; Shuai, Z. *Acc Chem. Res.* **1999**, *32*, 267−276. (b) Salzner, U.; Pickup, P. G.; Porer, R. A.; Lagowski, J. B. *J. Phys. Chem. A* **1998**, *102*, 2572−2578.
(9) (a) Greenham, N. C.; Moriatti, S. C.; Bradley, D. D. C.; Friend, R. H.; Holmes, A. B. *Nature* **1993**, *365*, 628−630. (b) Hanack, M.; Segura, J. L.; Spreitzer, H. *Adv. Mater.* **1996**, *8*, 663−666.
(10) Sotzing, G. A.; Thomas, C. A.; Reynolds, J. R.; Steel, P. J. *Macromolecules* **1998**, *31*, 3750−3752.
(11) Zong, K.; Reynolds, J. R. *J. Org. Chem.* **2001**, *66*, 6873−6882.
(12) Crystals of **10** were of low quality and lead to a rough structure with high *R* and wR values. The structure was reliable in terms of connectivity and atomic identity. It was also reliable in determining its overall shape and planarity.
(13) Sotzing, G. A.; Reynolds, J. R.; Steel, J. R. *Adv. Mater.* **1997**, *9*, 795−798.

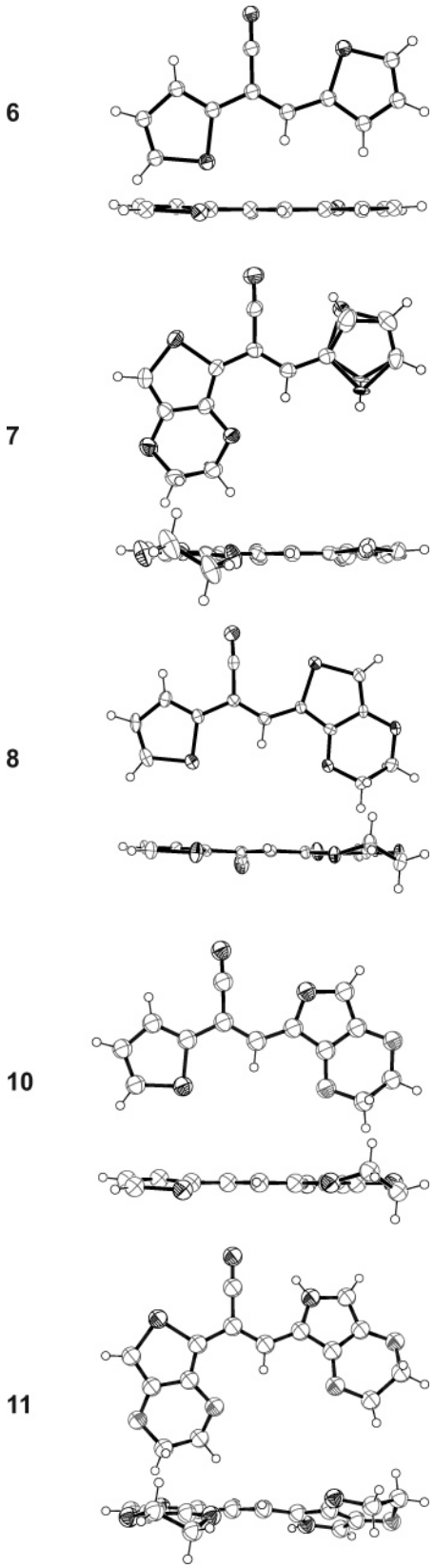

Figure 2. Monomer crystal structures for compounds **6**−**8**, **10**, and **11** indicate near-planarity for each molecule. Compound **9** did not crystallize.

noted that neither Th−Th, EDOT−EDOT, or mixtures of the two linkages have any known contraindications to planarity. Polymerization can be accomplished by a variety of oxidative electrochemical methods such as galvanostatic, potentiostatic,

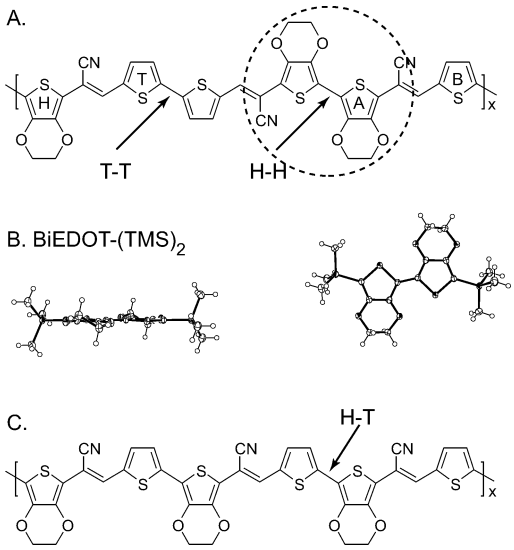

Figure 3. (A) Structure of (tail−tail) T−T and (head−head) H−H possibilities for PEDOT−CNV−Th electropolymerization. (B) Crystal structure of BiEDOT indicating planarity which corresponds to H−H coupling. (C) Schematic of regioregular PEDOT−CNV−Th composed solely of H−T couplings.

Table 1. Monomer and Polymer Fundamental Properties Derived from Monomer UV/Vis and Electrochemistry (potential in V vs SCE), as Well as Polymer Spectroelectrochemistry[a]

	monomer			polymer		
name	λ_{max}/nm	ϵ	E_{ox}	λ_{max}/nm	E_g/eV	E_1/nm
6	364	30 500	1.25	512	1.5	1100
7	378	21 600	1.10	531	1.4	1020
8	383	28 300	1.05	598	1.2	962
9	394	22 300	0.86	695	1.1	1100
10	394	29 100	0.83	642	1.1	1100
11	401	27 600	0.74	756	1.1	1396

[a] E_g is optical band gap and E_1 is the peak that is correlated to bipolaron presence in the UV−Vis NIR spectra.

or repeated scanning potential deposition and proceeds by chemical polymerization in O_2 for **11**, the most electron rich of the monomers.

The limiting potential, E_{ox}, from galvanostatic deposition at 10 μA on a 0.02 cm^2 Pt button in acetonitrile (ACN), 0.1 M tetra-*n*-butylammonium perchlorate (TBAP) for 250 s was used as a metric to determine polymerization potentials for potentiostatic deposition on IMEs and ITO glass electrodes. These potentials are shown in Table 1 along with a number of other relevant monomer and polymer properties. The limiting potential decreases throughout the monomer series **6**−**11** as monomer electron-rich character increases. The deposits obtained for all the polymers are all a quite similar light blue in the oxidized p-type doped state that darkens to a deep blue neutral state (*vide infra*). Because the oxidation potential for p-type doping of these polymers are all cathodic of the H_2O to O_2 redox couple,[14] they are all more stable in the p-type doped, transparent form and spontaneously dope over the course of several hours when left neutral under ambient conditions.

Spectroelectrochemistry. Band gaps (E_g) for CEPs are best determined by the onset of the π to π* absorption for the neutral form of the polymer determined from electronic spectroscopy,

(14) de Leeuw, D. M.; Simenon, M. M. J.; Brown, A. R.; Einerhand, R. E. F. *Synth. Met.* **1997**, 53−59.

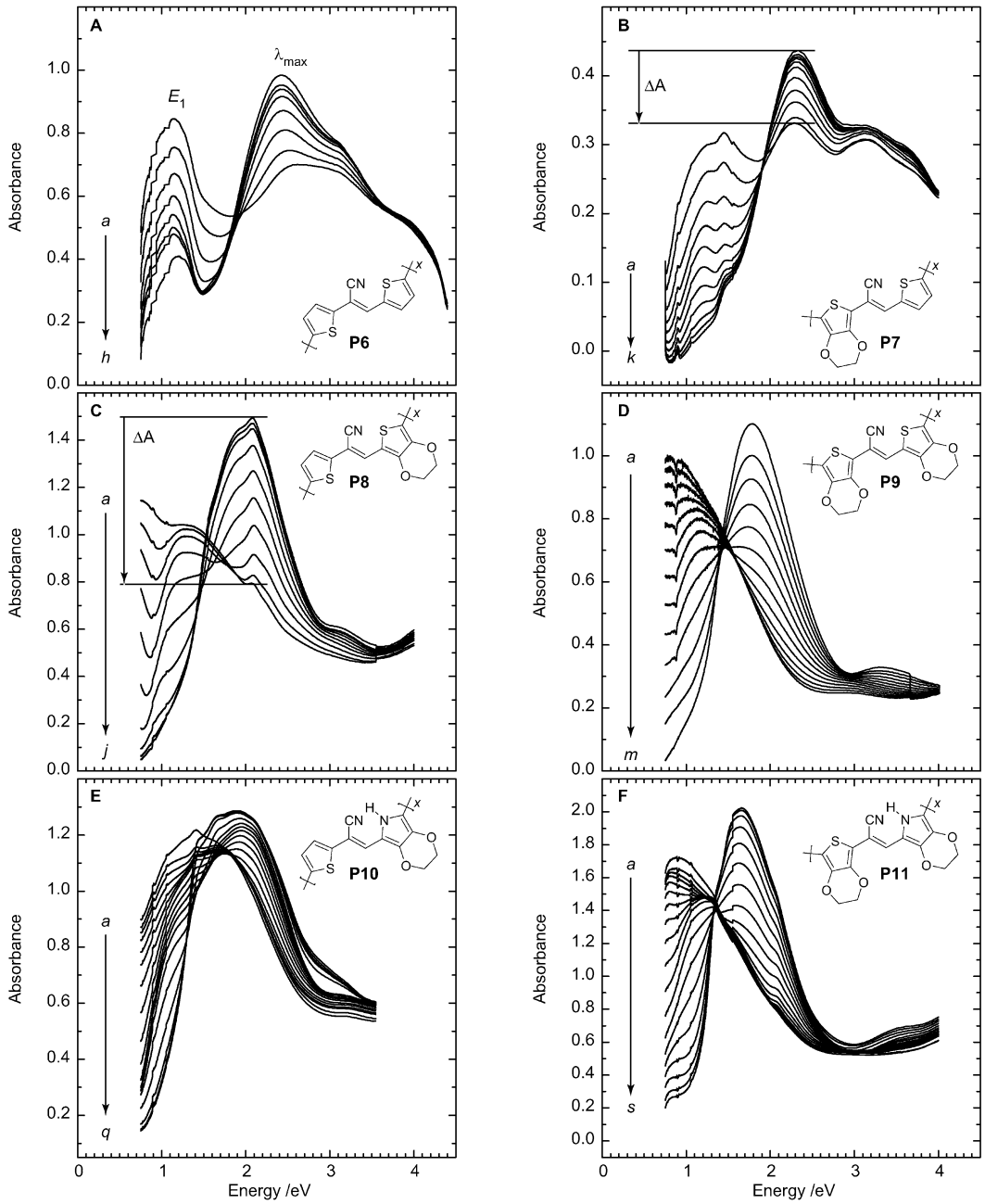

Figure 4. Spectroelectrochemistry in 0.1 M TBAP/ACN for cyanovinylene polymers electrochemically deposited to 25 mC cm^{-2}. (A) PBTh−CNV from $a = 1.53$ V to $h = -0.47$ V; (B) PEDOT−CNV−Th from $a = +1.03$ V to $k = +0.03$ V; (C) PTh−CNV−EDOT from $a = +1.33$ V to $j = +0.43$ V; (D) PBEDOT−CNV from $a = 0.98$ V to $m = -0.77$ V; (E) PTh−CNV−EDOP from $a = +1.23$ V to $q = -0.67$ V; (F) PEDOT−CNV−EDOP from $a = +1.23$ V to $s = -0.77$ V, all in 50 mV increments.

and the optical properties of these types of polymers have been treated in a number of reviews.[8] Monomers **6**−**11** were electropolymerized potentiostatically on ITO glass at a potential determined as described above to deposit polymer at a rate of *ca.* 1 mC cm^{-2} s^{-1} to a total charge of 25 mC cm^{-2} regardless of the exact rate. Figure 4 shows the spectroelectrochemical series for polymers **P6**−**P11** in degassed ACN 0.1 M TBAP. Polymer **P6** has been previously reported although the reported E_g differs from the one reported here substantially and has the highest E_g in this family of materials at 1.5 eV.[15] The oxidative spectroelectrochemistry for polymers **P6**−**P11** is similar and is characterized by an absorbance at low energy, *ca.* 1 eV, 1240 nm, and a larger peak between 2 and 3 eV attributed to the π to π^* transition and separated from the low-energy peak by an isosbestic point. Polymers **P6** and **P9** (Figure 4A,D) are related by the substitution of EDOT for thiophene in **P6**. This lowers the E_g from 1.5 to 1.1 eV, and the incorporation of EDOT in the polymer results in a more distinct π to π^* transition for **P9**. Polymers **P7** and **P8** (compare Figure 4B,C) are related by swapping the position of the thiophene and EDOT moieties relative to the cyano group. This change lowers the E_g from 1.4 (**P7**) to 1.2 (**P8**) and results in a greater absorbance change in the π to π^* region for **P8**. Polymers **P10** and **P11** incorporate EDOP in the B ring, and both have 1.1 eV band gaps with the

(15) Ho, H. A.; Brisset, H.; Elandaloussi, E. H.; Frére, P.; Roncali, J. *Adv. Mater.* **1996**, *8*, 990−994.

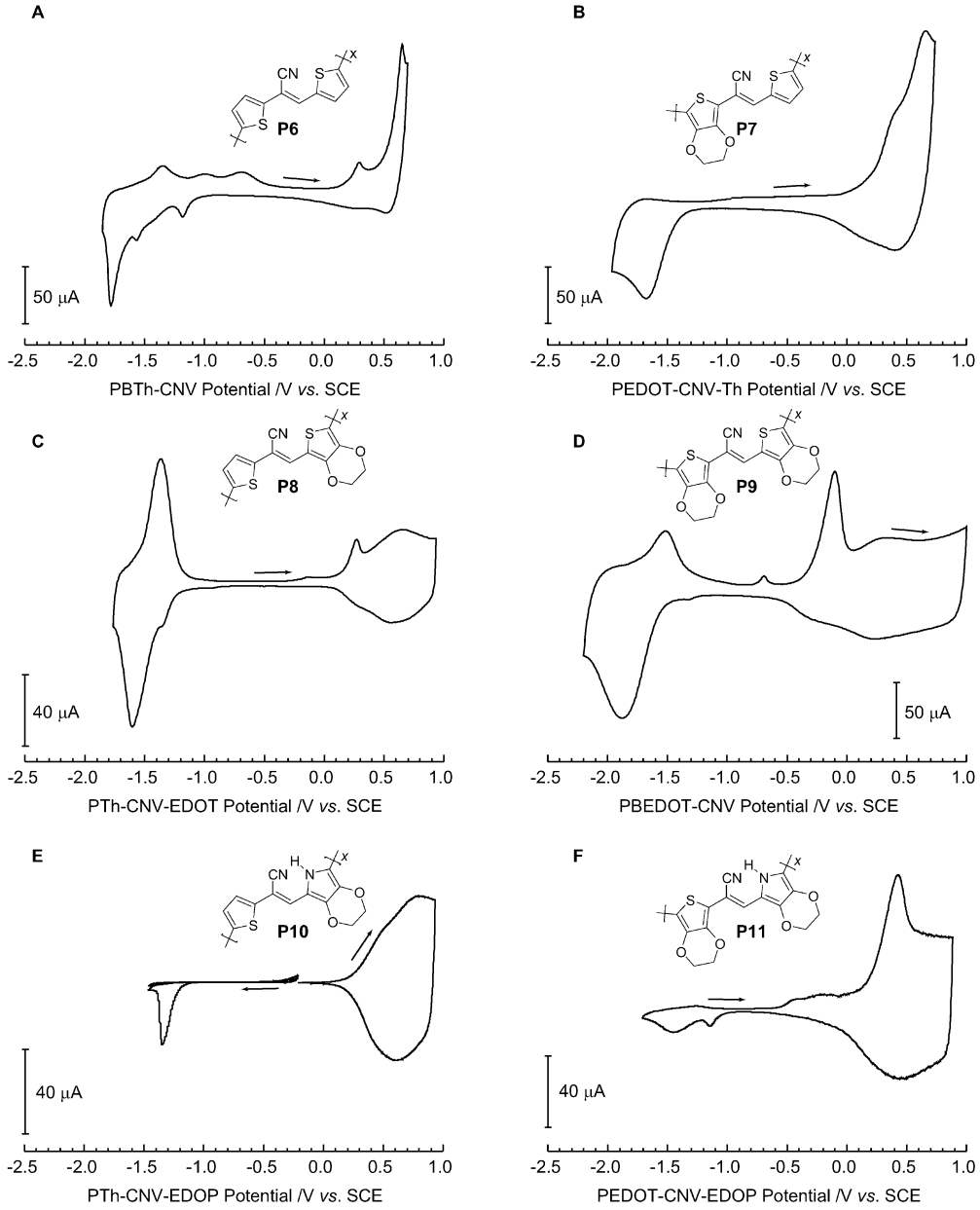

Figure 5. CV results for cyanovinylene polymers **P6**−**P11** in 0.1 M TBAP/ACN on a Pt disk electrode. All scans were started in a region where no electrochemical activity was present and were scanned first anodically to access the oxidative region and then cathodically to access the reductive electrochemistry.

P11 derivative showing an especially well-defined onset point as seen for polymers with near ideal switching properties.

Electrochemistry. There is a broad p-type doping process for each polymer which occurs at potentials in the range of 0.0 to +0.8 V vs SCE and is generally described by capacitive charging overlaying the faradaic polymer doping process as illustrated by the CV results in Figure 5. This broad oxidative process is coupled to an even broader charge neutralization process. Scanning cathodically of this oxidation/neutralization, a plateau is reached where very little current is observed. Even further cathodic scanning results in a new set of peaks commonly attributed to n-type doping of the polymer at potentials between −1.0 and −1.7 V vs SCE. Charge neutralization from the reduced form then occurs upon reversal of the scan direction.

Voltammetric studies to isolate the current response on p-type doping were performed by poising the polymer at a potential in the plateau region corresponding to the neutral form and scanning anodically. Exceptions to the typically broad oxidative wave are found in the two polymers that contain a thiophene in the ring B position, namely **P6** and **P7**. The oxidation peak for these polymers is quite sharp and occurs near 0.5 V vs SCE. **P10** (Figure 5E) is the exception to the above where the polymer oxidative and reductive voltammetric processes are separated to illustrate the instability of the cathodic process as evidenced by the degradation in the peak current value. On the first cathodic scan for this polymer, a small peak is observed at −1.4 V attributed to reduction of the polymer. On the subsequent return scan, this peak disappears due to the instability of the reduced polymer. This type of heightened sensitivity in the reduced form and decreased current responses in the reductive regions of the polymers which contain EDOP (**P10** and **P11**, Figure 5E,F, respectively) is typical as pyrrole-containing polymers are generally impossible to n-type dope. Despite the rela-

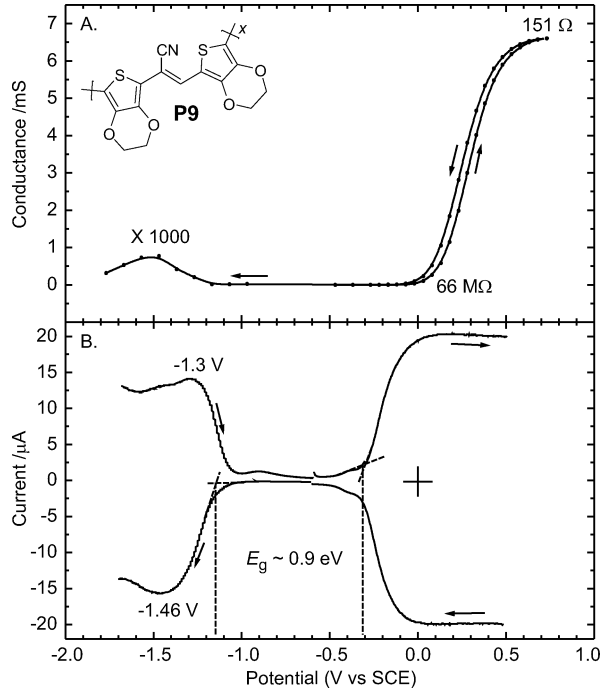

Figure 6. In situ conductance for PBEDOT−CNV on a 10 mm IME (A) and DPV on Pt disk (B) indicate an electrochemically derived band gap of 0.9 eV and a modest conductance upon reduction.

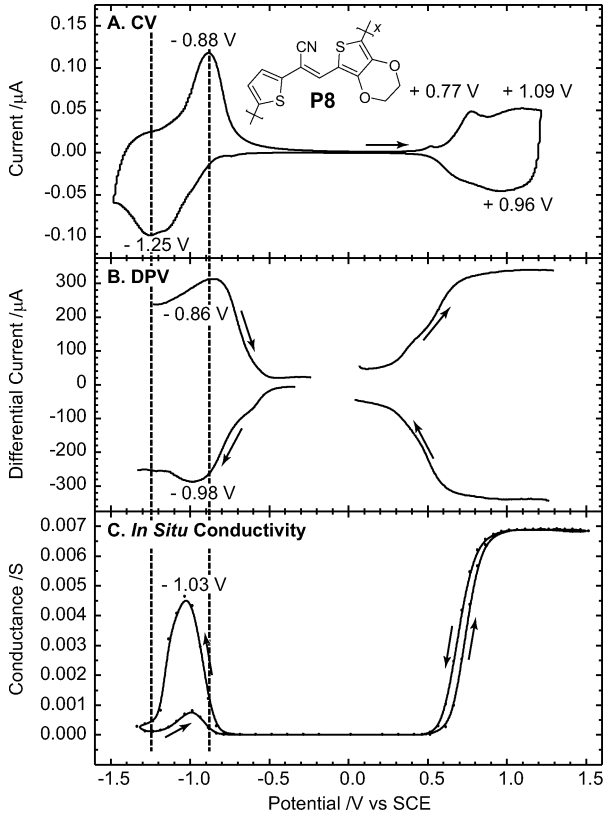

Figure 7. CV of PTh−CNV−EDOT film on IME (A), DPV on Pt (B), and in situ conductivity on IME (C). The peak in the in situ conductance plot correlates with the polymer E1/2 based on both CV and DPV results.

tively weak acidity of the pyrrollic proton, it is likely susceptible to acid−base chemistry by abstraction of that proton leading to another charged site on the polymer backbone. There is no analogous process in thiophene- or EDOT-containing polymers.

Stability upon oxidation/charge neutralization switching is excellent in these polymers, in general, with current stability over multiple hundreds of p-type switches exhibiting nearly zero decay. The stability to n-type switching was determined by the magnitude of the n-type peak current after several scans and is not as good as that for p-type doping. For **P8**, which was studied for an extended period of time, the peak currents decrease *ca.* 10% over the first 20 scans and then decrease only *ca.* 5% over the next 200 scans. Additionally, the shape of the reductive processes in **P8** and **P9** are the most symmetrical of all the polymers in this study, which indicates that there is little preference for ion transport in the doping or dedoping processes.

The *in situ* conductance and DPV results for **P9** are shown in Figure 6A,B, respectively. Increases in the conductivity occur for both oxidative (p-type) and reductive (n-type) doping. The p-type conductivity onset for **P9** is *ca.* 0 V vs SCE and occurs slightly more anodic of the corresponding peak in the DPV. The p-type conductance exhibits the typical S-shape.[16] The onset for n-type conductance occurs around −1.2 V vs SCE, giving this polymer a conductance derived band gap of 1.2 eV. This compares to the optical band gap of 1.1 eV and the DPV-derived band gap of 0.9−1.0 eV. The DPV results for **P9** mirrors the CV results in that the p-type doping processes appear quite broad in the CV and do not peak in the DPV.

Figure 7 shows the CV on an IME (Figure 7A), the DPV (Figure 7B) on a Pt button, and the *in situ* conductance (Figure 7C) on an IME for **P8**. The CV results on the IME are similar to the CV results in Figure 5 obtained on a Pt button. The DPV results are similar to those obtained for **P9**, where a broad p-type doping wave is observed that does not peak as in the comparatively sharper n-type DPV process. The DPV n-type to neutral transition (Figure 7B) wave peaks at nearly the exact potential as the corresponding CV process. In contrast, the neutral to n-type wave in the DPV experiment peaks at −0.98 V compared to the much more cathodic −1.25 V in the CV. For the *in situ* conductance plot (Figure 7C) a comparatively thick film was deposited in order to observe the n-type conductance more accurately. Under these conditions, the resistance of the p-doped polymer is sufficiently low to effectively short the IMEs so comparison of the p- and n-type conductance magnitudes is not possible. This results in a bell-shaped n-type conductance trace that is nearly symmetrical about the peak at −1.03 V vs SCE. Vertical lines drawn from the peaks in the CV trace would indicate that the peak in the n-type conductance and, indeed, all of the observable conductance in this range occur between the peaks in the CV. The n-type doping conductance experiment was duplicated after 72 h of storage in an Ar drybox, and the results are nearly identical to those in Figure 7C. This result indicates that very little degradation is evident in the polymer over this time scale and even less is to be attributed to the initial conductance experiment itself.

In addition to the two main redox processes available in this polymer family, there are several smaller peaks that occur inside the main oxidation process and the main reductive process. These peaks are more pronounced for samples of polymer that have been deposited under slow, more controlled conditions and,

(16) (a) Schiavon, G.; Sitran, S.; Zotti, G. *Synth. Met.* **1989**, *32*, 209−217. (b) Kittlesen, G. P.; White, H. S.; Wrighton, M. S. *J. Am. Chem. Soc.* **1984**, *106*, 7389−7396. (c) Paul, E. W.; Ricco, A. J.; Wrighton, M. S. *J. Phys. Chem.* **1985**, *89*, 1441−1447. (d) Thackeray, J. W.; White, H. S.; Wrighton, M. S. *J. Phys. Chem.* **1985**, *89*, 5133−5140.

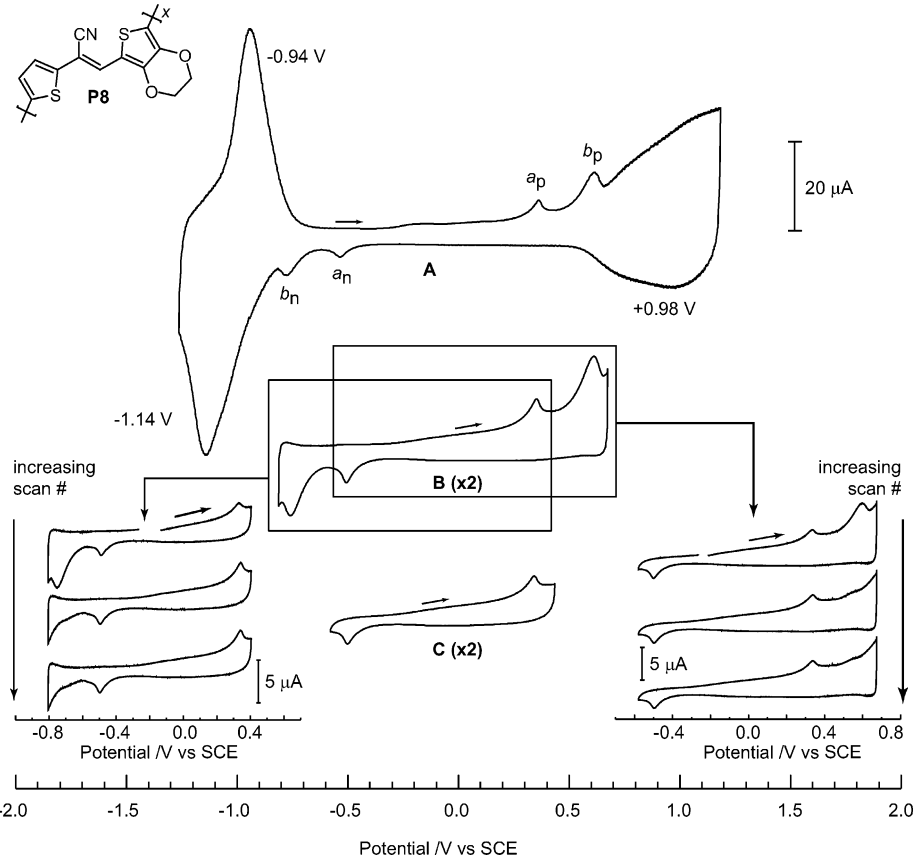

Figure 8. CV of PTh−CNV−EDOT on Pt disk showing oxidative and reductive doping as well as prepeaks a_n, a_p, b_n, and b_p (A). The prepeaks exist independently of the main polymer electrochemical processes (B). a_n and a_p exist independently of b_n and b_p (C).

as such, are presumed to be related to order in the polymer secondary structure. Figure 8 shows the cyclic voltammogram for **P8** deposited under these controlled conditions at a current of 10 μA (500 μA/cm^2). This polymer displays two sets of two peaks, dubbed prepeaks, inside of the main voltammetric processes. Some question about the exact nature of these prepeaks appears in the literature.[17] What is apparent is that prepeaks only appear after a reductive potential excursion. Repeated scanning over the p-type region does not result in the observance of prepeaks. Second, these prepeaks near the main anodic and cathodic voltammetric processes are correlated to each other. That is, the outer two peaks, labeled b_n and b_p in Figure 8 and the inner two peaks, labeled a_n and a_p are coupled and do not exist unless a potential more cathodic or more anodic of the peak is accessed during cycling. Figure 8C illustrates the coupled nature of the inner set of prepeaks. Figure 8B partially illustrates the coupled nature of the outer set of prepeaks, but the callouts further clarify this. The callout on the left shows three sequential cyclic voltammograms over the region of b_n, a_n, and a_p. On the first scan b_n is visible but is absent from the second two scans, indicating that it is necessary to access b_p in order for b_n to appear on subsequent scans. The complement to these results is shown in the callout on the right side of Figure 8. In this series of voltammograms, the potentials where a_n, a_p, and b_p appear are accessed, and while b_p appears on the first scan, it does not appear on the second or subsequent scans when b_n is not accessed.

Scan rate dependence experiments for **P8** exhibit the typical linear dependence on scan rate expected for an electrode-adhered film over the scan rates where doping is not diffusion-limited. This occurs up to 500 mV s^{-1} for **P8** and deviates from perfect linearity only due to polymer break-in over the first 30 scans, an observation that is consistent with reports that n-type doping break-in takes more scans than p-type doping break-in at approximately 40−50 scans and 10−20 scans, respectively.[17a] This scan rate linearity occurs over a much broader range of scan rates than the typical homopolymers of pyrrole, thiophene, and EDOP that make up these polymers excluding PEDOT, which demonstrates exceptional linear scan rate dependence.

Experiments to probe the countercation tolerance were also performed. A film of **P8** was deposited from a solution of TBAP. Assuming anion dominant ion transport for p-type doping, this resulted in a film containing perchlorate. CV results were then collected over 10 scans with TBAP, TEAP, and finally $LiClO_4$. The polymer stability in TBAP is discussed below. Peaks associated with n-type doping when TEAP or $LiClO_4$ were involved decreased rapidly and were not observed again even upon return to TBAP. This type of behavioral instability correlates with the results we have observed with pyridine/pyridopyrazine acceptors as well.

Colorimetry. Although the band gaps for this family of polymers changes over a range of 0.4−0.5 eV, they are quite similar in terms of the qualitative color transitions that they undergo. This is attributed to the fact that these electronic transition modifications are mainly occurring in the near-IR portion of the spectrum. Films on ITO change from a moderate,

(17) (a) Zotti, G.; Schiavon, G.; Zecchin, S. *Synth. Met.* **1996**, *72*, 275−281. (b) Crooks, R. M.; Chyan, O. M.; Wrighton, M. S. *Chem. Mater.* **1989**, *1*, 2−4. (c) Borjas, R.; Buttry, D. A. *Chem. Mater.* **1991**, *3*, 872−878.

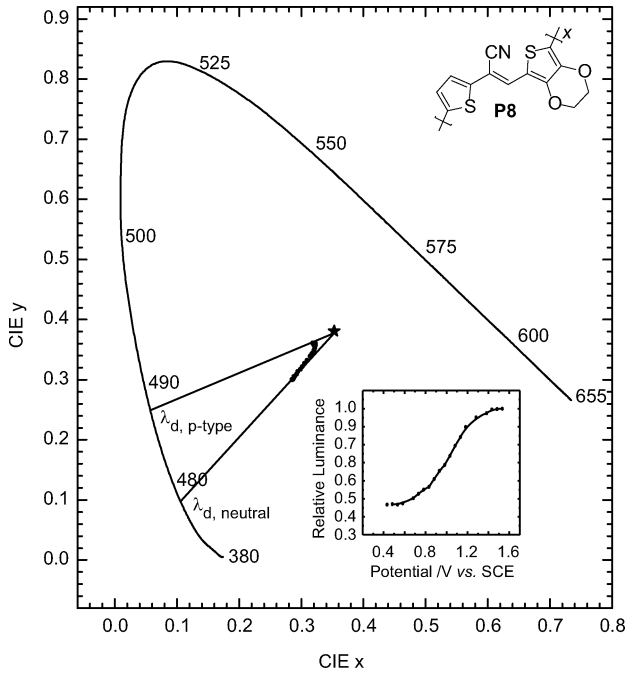

Figure 9. Colorimetry (relative to CIE 1931 standard observer) for a PTh−CNV−EDOT film during p-type doping−dedoping undergoing a color change from pale blue to deep blue.

absorbing blue (undoped state) to a transparent light blue (p-type conducting). The transparency of the light blue undoped state appears greater to the eye for **P8** and **P9** than for the other polymers. The color changes during the p-type to neutral transition are illustrated quantitatively in Figure 9 for **P8**. The inset to Figure 9 shows the luminance as a function of potential and indicates that to the eye, the polymer undergoes a 50% change in luminance over its doping range.

Discussion and Conclusions

The use of the Knoevenagel condensation for the preparation of the cyanovinylene acceptor core proceeds in yields of 80−95%. Historically, overall synthetic yields for D−A monomers have often been hampered by the need to cross-couple two aromatic heterocycles with the concomitant loss in yield for the preparation of organo−tin, −ZnCl, or −boronate reagents and the coupling reactions used in Stille, Negishi, and Suzuki reactions. The method used here lessens some of the complications of combining premade D−A units and eliminates the need for expensive and toxic tin reagents completely while placing the lower yielding synthetic steps early in the monomer synthesis. As such, we have been able to attain a set of D−A−D electropolymerizable monomers which yield a family of polymers where comparison of the backbones symmetry and electron-rich character is possible.

The electropolymerization possibilities must be addressed before there is a discussion of its effect on the electronic structure.[18] Upon electropolymerization, each polymer is well-adhered to the electrode surface and insoluble in both its oxidized and reduced forms as desired for a highly electroactive polymer. Determining the actual amounts of H−T, H−H, or T−T couplings illustrated in Figure 3 is thus not possible; however, some hypotheses exist. It is anticipated that one-electron oxidation of a monomer in this family removes an electron from the HOMO which is presumably located on the heteroatom (S or N) of the most electron-rich heterocycle. This cation radical then rearranges to place the highest spin density predominantly at the 5 position (the site immediately adjacent to the heteroatom but not connected to the remainder of the molecule) of the heterocycle, which then undergoes dimerization as described for symmetrical monomers such as thiophene, pyrrole, EDOT, and EDOP.[19] This dimerization presumably occurs with another radical cation where the spin is similarly located primarily on the 5 position of the most electron-rich heterocyclic moiety since this is the radical species that is anticipated to occur in the highest concentration early in the electropolymerization. Assuming that the radical can be located on the most electron-rich heterocycle with some certainty, this produces a H−H or T−T dimer, depending on whether the electron-rich heterocycle is nearer the cyano group or not.

From here multiple options exist for the formation of the polymer. First, the extended conjugation dimers will have lower oxidation potentials than the original monomers and likely oxidize next, encounter additional molecules of the initially described radical cation, and form the first H−T coupling in the ensuing trimer. The electrochemical deposition of **10** is slightly different from the other monomers studied in that preparation at low current densities leads to open morphological, nodular films that do not fully cover the electrode surface, rather than the smooth polymer films that rapidly deposit for the other monomers electropolymerized under identical conditions. As **10** has the greatest difference in electron-rich character between the two heterocycles, we surmised that there was a potential floor, below which the T−T dimer (thiophenes on the perimeter of the dimer) would not be oxidized and only this dimer would be formed. Semiempirical calculations on the monomer, H−H, T−T, and H−T dimers on **10** were used to test this hypothesis. Using orbital energies from PM3 calculations (ϵ_{HOMO}), Koopmans' theorem,[20] and a correction factor from vacuum to SCE which includes a solid-state polarization parameter,[21] the ionization potentials (IP) were estimated for these dimers and the monomer.[22] Koopmans' theorem simply states that the ionization potential can be derived from the HOMO energy, while a solid-state polarization correction is necessary to first convert the potential reference from the vacuum level to SCE and second to take into account the nonspecific solid interactions that differentiate the actual dimer energy from the vacuum calculations. While the experimentally determined values (Table 1), as compared to the Koopmans' estimated values, are different for the systems by about 1 V, trends in the calculations indicate that every possible dimer formed has a lower oxidation potential than the monomer. The most surprising result of these calculations (see Supporting Information) is that, for all the dimers of **10**, the H−H dimer (with EDOPs on the periphery) has the highest oxidation potential. This could be the result of facile oxidation of the electron-rich $(EDOP)_2$ unit at the core of the T−T dimer, rather than the terminal heterocycle as proposed in the mechanism outlined above. This may result in spin

(18) Hutchison, G. R.; Zhao, Y.-J.; Delley, B.; Freeman, A. J.; Ratner, M. A.; Marks, T. J. *Phys. Rev. B* **2003**, *68*, 35204-1−325204-13.

(19) Marynick, D. S.; Reynolds, J. R. *Polym. Prepr.* (*Am. Chem. Soc., Div. Polym. Chem.)* **1992**, *33*, 1158−1159.

(20) Koopmans *Physica* **1933**, *1*, 104−113.

(21) Brédas, J. L.; Heeger, A. J. *Macromolecules* **1990**, *23*, 1150−1156.

(22) Micaroni, L.; Nart, F. C.; Hummelgen, I. A. *J. Solid State Electrochem.* **2002**, *7*, 55−59.

localization on the interior of the monomer distant to where it needs to be to productively form polymer. These results suggest that the slow deposition and poor film quality of **P10** is due to poorly matched oligomer solubility with solvent conditions or poor coupling of the T−T dimer from spin localization, rather than the existence of a potential floor which limits oligomer growth from dimer. Since the other monomers are all more closely matched in terms of flanking heterocycle electron-rich character, the idea that all dimers have lower oxidation potentials than the monomers appears to be a generally valid assumption for this monomer family.

The spectroelectrochemical series shown in Figure 4 for all of the polymers shows the effect of increasing the electron-rich character of the donor heterocycle about the cyanovinylene on lowering band gap, but does not explain how this occurs. Contention over the optoelectronic properties of **P6** exists as its band gap was initially reported to be 0.8 eV,[15] the event which initially drew our attention to this family. The subsequent resynthesis and characterization for this work and substantiated by others[23] confirms that the polymer in the original study was not completely reduced prior to estimation of the band gap from the spectrum of the neutral polymer alone, resulting in a shoulder at lower energy being taken for the band gap. As this polymer was the first to be synthesized in this family, it reflects some of the liabilities of this system, namely, **P6** has the highest oxidation potential for all of the polymers in this family (Figure 4A) and is the most difficult material to reduce completely. The spectrum for the neutral polymer (Figure 4A, curve h) represents a polymer that has first been electrochemically, and subsequently chemically reduced by addition of *ca.* 0.25 mL of hydrazine to 2 mL of solvent and electrolyte. Despite these rather forcing reducing conditions, **P6** still shows evidence of charge carriers present in the form of the peak E_1 at 1.2 eV. Exchanging the thiophenes in **P6** for EDOT, **P9** is easily neutralized electrochemically as evidenced by a clean absorption onset at *ca.* 1 eV and single peak at 1.7 eV. Upon oxidation, the π to π^* is fully bleached, while the strong charge carrier absorption, found mainly in the near-IR, extends out past 2 eV. A well-defined isosbestic point is also present, which is taken as evidence that the polymer undergoes a state-to-state transition between the p-type doped and neutral forms. The band gap for **P9** is *ca.* 1.1 eV, 0.4 eV lower than **P6**, resulting in a reduction of λ_{max} from 512 to 695 nm. **P9** also undergoes a much more significant optical switching absorption change in the visible and near-IR spectral regions compared to **P6** as would be desired should this polymer be considered for electrochromic applications.

Comparison of the spectroelectrochemical results for the two monomers containing one EDOT and one thiophene allows us to examine the effect of switching the position of the heterocycles about the cyanovinylene group. This exchange leads to a decrease in band gap of ca. 0.2 eV from **P7** to **P8**. This effect is evident in both the absorption onsets, which are sometimes difficult to determine exactly, and the λ_{max} value, which is more concrete. Similar to the polymers **P6** and **P9** above, the polymer with an EDOT group not directly adjacent to the cyano group shows improved spectral properties in the sense that **P8** undergoes greater optical switching depth and displays a more well-defined band in the near-IR that is attributed to E_1. In Figure 4C representing **P8**, the ΔA at λ_{max} is 0.7 absorbance units, where, in the spectra for **P7** (Figure 4B), the ΔA is only 0.1 absorbance units. Recall that these films are all synthesized to the same charge density. Because of the above properties and the well-defined electrochemistry, facile monomer synthesis, and good stability, **P8** represents one of the most useful polymers in this family.

Interestingly, further increasing the electron-rich character of the heterocycle flanking the cyanovinylene group does not continue to decrease the band gap. The band gaps of **P10** and **P11** saturate at 1.1 eV with **P11**, giving the cleanest absorption onset and isosbestic point for the full family of polymers. The spectroelectrochemical series for **P10** shows a broad π to π^* transition and very little switching change through the visible region, possibly due to film morphology from the nonstandard film forming characteristics mentioned previously. An additional comment is worth presenting concerning the monomer stability of the pyrrole containing members of the family. Compound **10** is also the monomer with the greatest differential in electron-rich character of the heterocycles around the cyanovinylene. While solutions of the **10** monomer in ACN/TBAP tend to be moderately stable, there is slight discoloration after standing capped for several days. Solutions of **11** on the other hand, capped under argon become completely dark after standing for only hours. This observation lends further credence to the theory regarding stability of the T−T coupled dimer.

Spectroelectrochemistry was attempted in the potential region in which n-type doping would be expected. These results showed that there was no observed change in spectral signature for any of the polymers before polymer degradation was evident. This is presumably due to one of two possibilities. First, sealing of the cell used to perform p-type to neutral spectroelectrochemistry is likely inadequate for the more rigorous demands imposed by reduced polymers. At the same time, changes in optical characteristics in the drybox were not evident to the eye for these polymers upon reduction even though the corresponding electrochemical processes are easily documented and are quite stable. These experiments were performed with the same equipment and methodology used to identify color changes in similar systems with pyridine as the acceptor and underscores our position that electrochemical response in the cathodic region is insufficient to confirm the formation of delocalized charge carriers.[7] This suggests the possibility that, even though charges are created on the polymer chain with the concomitant ion transport associated with doping, mobile charge carriers are not produced and thus no color change occurs.

Examination of the set of cyclic voltammograms in Figure 5 shows the major oxidative and reductive processes, along with a series of smaller prepeaks. The physical intuition for prepeaks is that they are due to trapped charge in the polymer. When **P8** is oxidized (held at *ca.* +1.0V), then charge compensated to the neutral form, there remain sites that are still oxidized where the dopant is either trapped in the polymer or there is a surface or near-electrode interaction that prohibits this section of polymer from being charge-neutralized. As the potential is scanned more negative, these sites a_n and b_n as described in Figure 8 are neutralized. The polymer n-type doping neutral to anionic transition is observed on scanning more cathodic of the

(23) Moratti, S. C.; Bradley, D. C.; Cervini, R.; Friend, R. H.; Greenham, N. C.; Holmes, A. B. *Proc. SPIE Int. Opt. Eng.* **1994**, *2144*, 108−114. (b) Moratti, S. C.; Cervini, R.; Holmes, A. B.; Baigent, D. R.; Friend, R. H.; Greenham, N. C.; Gruener, J.; Hamer, P. J. *Synth. Met.* **1995**, *71*, 2117−2120.

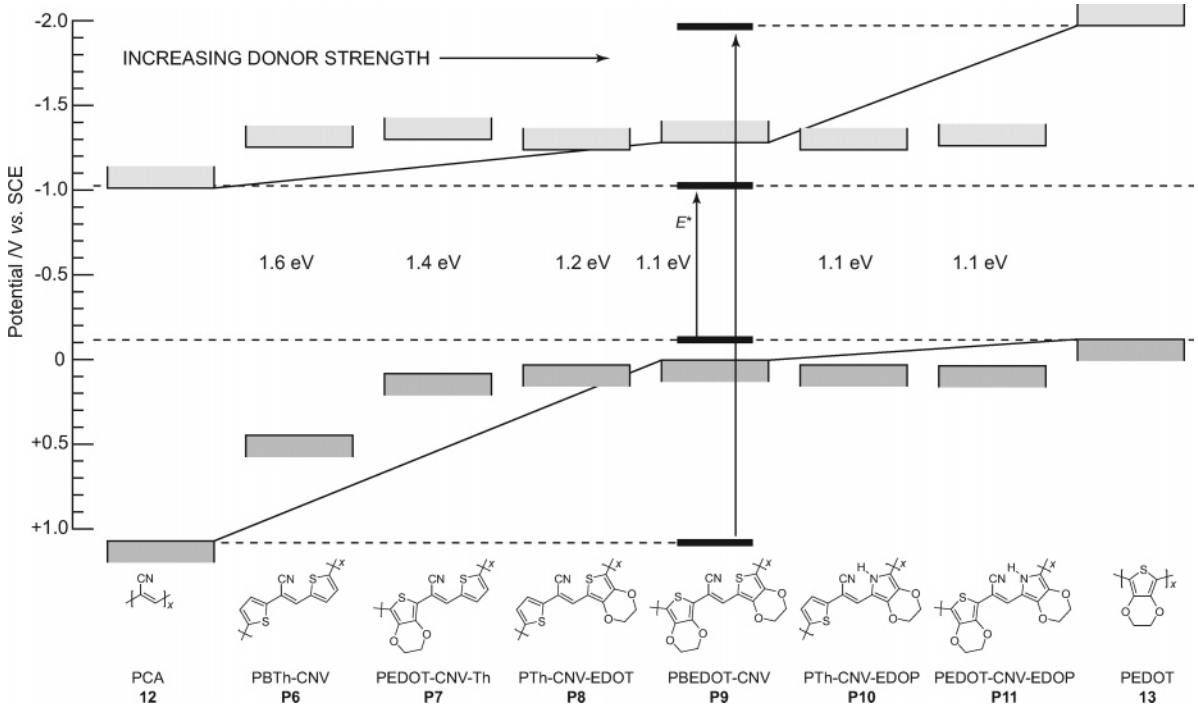

Figure 10. Approximate levels of frontier bands for pure acceptor (PCA) through pure donor (PEDOT), showing the effect of increasing donor strength in a D−A−D configuration. (PCA provided by Chris Gorman at NC State).

prepeaks. On the return anionic-to-neutral transition, trapped anionic charge states are not neutralized until a_p and b_p are scanned. The prepeaks can be quite large compared to the actual polymer doping process as seen in Figure 5D for **P9**.

Combination of the results attained throughout this study allows a relatively complete picture of the electronic properties of this family of polymers to be constructed and compared. Figure 10 shows this where the primary energy of the band onsets are derived from CV and are checked against *in situ* conductance results when available. Despite the combination of thermodynamic and kinetic data in the CV results possibly obscuring the desired thermodynamic information, in this particular family of polymers the CV results correlate with the spectroscopic results more closely than DPV. Higher priority is placed on conductivity results than CV onsets and absolute determination of the band gap is made using the spectroscopic results. When spectroelectrochemical results contradicted CV results, the baricenter of the band gap was determined by CV and the band gap magnitude was superimposed upon this to get the valence band (VB) and conduction band (CB) onsets. In all cases, CV slightly overestimates the band gap when the onsets are not obscured by prepeaks. DPV results slightly underestimate the band gap and conductivity results come the closest to corroborating spectroelectrochemical results while providing added information about band edges in energy space. DPV results are quite sensitive to any sort of ion transport process resulting from redox chemistry, and in general the differential currents change over 2 orders of magnitude. Conductance results often change over 5−7 (or greater) orders of magnitude and measure the contribution from redox chemistry to conductivity only. This allows a partial explanation of why the DPV and conductivity results do not match exactly. While the DPV trace is beginning to rise, there is very little contribution to the conductivity that is visible on a linear scale, and thus the conductivity appears to lag the DPV.

From Figure 10 it is apparent that the narrowing of the band gap is entirely the result of the VB being raised in energy with increased electron-rich character of the heterocyclic component while the CB remains fixed. This is in accord with the premise of this work, that the VB energy is set by the identity of the donor while the CB energy is set by the identity of the acceptor. Given the scope of donor and acceptor moieties in this work, there appears to be a lower limit to the band gap that can be achieved by simply increasing the electron-rich character about a single acceptor. Ultimately, a band gap of 1.1 eV was achieved whether EDOT was used alone or a combination of thiophene, EDOT, and the much more electron-rich EDOP was used. An argument can be made that the ultimate example of the electron-rich heterocycles in this study around the cyanovinylene core (**11**) is not truly the lowest band gap that can be demonstrated by this system due to the considerable deviation from planarity (*ca.* 25°) in this particular monomer. If one is simply trying to obtain the lowest band gap material, attention to the details that cause **11** and future monomers based on EDOP to diverge from planarity is necessary. However, given the synthetic complexity of EDOP synthesis (relative to the commercial availability of EDOT) and the incorporation of EDOP into other systems due to the difficulty in activating EDOP for reaction at the 2-position and preparing protected analogues of EDOP, it is evident that the desired properties can be attained using the EDOT family. Indeed, the fully substituted EDOT system (**P9**) appears to be the best compromise in terms of maximum donor strength and ease of synthesis. EDOT is far more stable as a monomer than EDOP, is easily functionalized at the 2-position (lithiation, stannylation, formylation, etc.), and provides polymers which are easily reducible when incorporated into monomers with an acceptor.

The issue of reduction bears further comment. One of the main driving forces behind low band gap CEP research has been to make available materials that n-type dope in an accessible

potential region. Taking into account the reduction potentials for oxygen and water, while allowing for common overpotentials, places the need to have a polymer n-type dope at a currently inaccessible −0.5 V vs SCE to be stable in air.[14] It appears that a reduced polymer containing EDOP would not be stable in devices regardless of this presently out of reach potential target.

Despite a reduced band gap, the all-thiophene- and all-EDOT-containing polymers exhibit unimpressive n-type conductivities. This situation arises presumably from the necessity to use TBA^+ as a dopant cation rather than the smaller and more n-type compatible TEA^+ or Li^+. Use of either of these alternative cations leads to rapid polymer degradation. The use of TBA^+ electrolytes creates a scenario where the conductivity rises a small amount and falls back to nearly zero within the confines of the doping processes determined by CV. This strongly implies that the total conductivity upon reduction, which is the sum of the electrical conductivity and the redox conductivity, is dominated by the redox conductivity, that is, the conductivity derived from the gate potential forcing the polymer to be partially doped. In a polymer system suitable for n-type devices, the polymer architecture must be engineered to tolerate smaller, more mobile dopant ions so that the electronic conductivity dwarfs the conductivity derived from mixed-valent states along the polymer backbone as occurs with p-type doping. A fundamental requirement of conductivity matching also appears necessary where the n-type and p-type conductivities are within an order of magnitude of each other. In these systems, the n-type conductivity is generally 4−5 orders of magnitude less than the p-type conductivity.

Acknowledgment. We gratefully acknowledge funding of this work from the AFOSR (Grant F49620-03-1-0091) and the ARO/MURI program (Grant DAAD19-99-1-0316). We also acknowledge Chris Gorman (North Carolina State University) for providing the sample of poly(cyanoacetylene) used to determine frontier orbital positions in Figure 10 and initial contribution to this work by Dr. Greg Sotzing (University of Connecticut).

Supporting Information Available: Full experimental details and crystallographic studies, along with monomer UV/vis spectra and calculated ionization potentials (PDF, CIF). This material is available free of charge via the Internet at http://pubs.acs.org.

JA048637W